

Dynamical black holes & expanding plasmas

Pau Figueras^{a*}, Veronika E. Hubeny^{a,b†}, Mukund Rangamani^{a,b‡}, and Simon F. Ross^{a§}

^a*Centre for Particle Theory & Department of Mathematical Sciences,
Science Laboratories, South Road, Durham DH1 3LE, United Kingdom.*

^b*Kavli Institute for Theoretical Physics,
University of California, Santa Barbara, CA 93015, USA.*

March 23, 2009

Abstract

We analyse the global structure of time-dependent geometries dual to expanding plasmas, considering two examples: the boost invariant Bjorken flow, and the conformal soliton flow. While the geometry dual to the Bjorken flow is constructed in a perturbation expansion at late proper time, the conformal soliton flow has an exact dual (which corresponds to a Poincaré patch of Schwarzschild-AdS). In particular, we discuss the position and area of event and apparent horizons in the two geometries. The conformal soliton geometry offers a sharp distinction between event and apparent horizon; whereas the area of the event horizon diverges, that of the apparent horizon stays finite and constant. This suggests that the entropy of the corresponding CFT state is related to the apparent horizon rather than the event horizon.

*pau.figueras@durham.ac.uk

†veronika.hubeny@durham.ac.uk

‡mukund.rangamani@durham.ac.uk

§S.F.Ross@durham.ac.uk

Contents

1	Introduction	1
2	Boost invariant flow	5
2.1	Bjorken hydrodynamics	5
2.2	The gravity dual to Bjorken flow	6
2.3	Apparent horizon for the BF spacetime	9
2.4	Event horizon for the BF spacetime	10
3	The Conformal Soliton flow	13
3.1	The BTZ spacetime as a conformal soliton	13
3.2	Event horizon for the CS spacetime	15
3.3	Event horizon area & field theory entropy	18
3.4	Apparent horizon for the CS spacetime	22
4	Discussion	23
A	Conformal solitons in higher dimensionss	26
B	The conformal soliton flow and hydrodynamics	28
C	Apparent horizon in the Poincaré slicing of BTZ	30
D	Apparent horizon coincides with Killing horizon	32

1 Introduction

The AdS/CFT correspondence has over the years played an invaluable role in providing insight into the dynamics of strongly coupled gauge theories. An important application of the correspondence has been to understand the holographic description of hydrodynamic properties of field theories. This can be used to understand qualitative features of the Quark-Gluon plasma (QGP) produced in heavy ion collisions. Current theoretical understanding

of this system is that subsequent to rapid thermalization, the system evolves as an almost ideal fluid, expanding rapidly away from the central collision region. The evolution in this regime has been well described by the so called Bjorken flow [1].

The first step in understanding the holographic dual of the Bjorken flow was taken in the seminal works [2, 3], where the spacetime dual to the Bjorken flow in $\mathcal{N} = 4$ Super-Yang Mills was constructed as a perturbation expansion at late times (see [4] for recent review summarising the development of the holographic description of the boost invariant plasma). This geometry models the early (but post-thermalization) stages of the expanding quark gluon plasma.

More generally, given any interacting quantum field theory, one can study its hydrodynamic regime. A natural question in the context of the AdS/CFT correspondence is whether this regime admits a holographic dual spacetime. This was answered in the affirmative in [5], where the authors proposed the *fluid-gravity correspondence* relating the dynamics of the field theory fluid to gravitational dynamics of black holes in an asymptotically AdS spacetime. The fluid-gravity correspondence generalizes the extensive discussion of hydrodynamics of field theories with gravitational duals¹ and explicitly constructs spacetime geometries dual to fluid flows in the hydrodynamic regime; that is, for cases where the fluid remains in local thermal equilibrium. This provides a useful relation between the dynamics of strongly coupled systems in the long-wavelength regime and corresponding asymptotically AdS black hole geometries. It provides a new approach to the calculation of properties such as transport coefficients of the field theory fluid.

In general, the flow of a viscous fluid, which involves dissipation, necessarily leads to entropy production. This of course is a simple consequence of the second law of thermodynamics. In the geometric description of the fluid flow one can ask what this phenomenon of entropy production corresponds to. An important ingredient in the fluid-gravity correspondence was the identification of the global event horizon in the bulk spacetime, which turned out to provide a simple geometric construction for a Boltzmann H-function in the bulk geometry. It was shown in [16] that the event horizon in the spacetimes dual to non-linear fluid flows could be determined essentially locally despite the teleological nature of event horizons. This was achieved by assuming slow temporal variations, as well as that the geometry will settle down to a stationary configuration at late times (which is of course natural from the fluid dynamical point of view, as one expects the dissipative effects of viscosity etc., to cause the fluid motion to slow down asymptotically and the system to achieve global equilibrium). The location of the event horizon is then given by a perturbation around this final equilibrium position. The perturbed position of the horizon can be determined order by order in the derivative expansion. The area-form of this event horizon when pulled back

¹For a review and references to earlier works on hydrodynamic aspects of $\mathcal{N} = 4$ Super Yang-Mills see [6]. Extensions of the fluid-gravity correspondence to include forcing and charge transport have been considered in [7, 8, 9, 10, 11, 12, 13, 14, 15].

to the boundary was shown to lead to a natural local entropy current with non-negative divergence as required by the second law.

Our main aim in this paper is to extend this work to determine the location of the horizons in certain time-dependent geometries that do not settle down to stationary finite-temperature solutions at late times. Our interest in this question originally arises from the Bjorken flow (BF) geometry, but we will also consider the conformal soliton (CS) geometry, which provides a simpler example with stronger time dependence.

For the Bjorken flow, explicitly constructing the event horizon will allow us to confirm the regularity of the bulk geometry. In [2, 3], the geometry was constructed as a perturbation expansion in the boundary time coordinate which is valid at late times. By demanding regularity of the solution at leading orders, the authors were able to derive the transport properties of the plasma, most notably the shear-viscosity η which saturates the famous bound $\eta/s \geq 1/4\pi$ [17]. The study of the gravitational dual at higher orders was undertaken to derive the relaxation time of the plasma in [18, 19]. However, the regularity of the dual spacetime was brought into question as subleading singularities were encountered [18, 20]. This issue was addressed recently in [21, 22] where the authors used the framework of the fluid-gravity correspondence [5] to argue that the spacetime was indeed regular. We will revisit this analysis and confirm regularity by explicitly constructing the global event horizon for these geometries. Previously, [22] found the apparent horizon in the BF geometry, as an approximation to the event horizon; here we confirm that the actual event horizon indeed closely tracks the location of the apparent horizon.² Since the Bjorken flow does not settle down to a finite-temperature stationary state, we determine the event horizon by explicitly constructing the boundary of the past of the future null infinity \mathcal{I}^+ .³ Curiously, we find that the apparent horizon lies outside the event horizon at the leading order in the perturbation expansion. This simply reflects the fact that the leading order metric violates energy conditions. At first order the event horizon overtakes the apparent horizon and the situation becomes more conventional.

The conformal soliton geometry [24] provides a simpler example, where we can gain intuition about more general fluid flows. It is simply a patch of the well-known Schwarzschild-AdS black hole, so the explicit metric is known exactly, and admits a high degree of symmetry. Nevertheless, if we work in a coordinate system corresponding to considering the field theory on flat space $\mathbf{R}^{3,1}$ rather than the Einstein static universe $\mathbf{S}^3 \times \mathbf{R}^1$, taking a ‘Poincaré patch’ of the Schwarzschild-AdS black hole, the time translation symmetry is no longer manifest,

² Here we will take “apparent horizon” to mean the full co-dimension 1 surface in the spacetime rather than just a co-dimension 2 slice of that surface; please see the Note added in v2 at the end of Discussion for a clarification of the quasilocal horizon jargon. We thank Roberto Emparan for valuable discussions on these issues.

³The future null infinity \mathcal{I}^+ corresponds to ‘endpoints’ of future-directed null geodesics and is timelike for asymptotically AdS spacetimes.

and the solution looks highly dynamical. Pictorially, it corresponds to a black hole entering through the past Poincaré horizon and exiting through the future Poincaré horizon, with its closest approach to the boundary occurring at $t = 0$ (Poincaré time). In the boundary CFT, this describes a finite energy lump which collapses and re-expands in a time-symmetric fashion. Here the hydrodynamic approximation is not valid at all times, but because this fluid flow is conformal to a stationary fluid on the Einstein static universe, the stress tensor is shear-free; that is, there is no dissipation in this fluid flow.

The horizons in this case are more interesting. Naively one might expect that since we are just performing a coordinate transformation on a given solution, any geometrical feature, such as the location of the event horizon, remains invariant under such a transformation. In other words, we might expect that the event horizon of the Poincaré patch of Schwarzschild-AdS black hole coincides with the event horizon of the global Schwarzschild-AdS. However, as we argue below, this is not the case, because our coordinate patch now includes only part of the future infinity of the global Schwarzschild-AdS. As a result, the actual event horizon for the conformal soliton lies outside the global event horizon of Schwarzschild-AdS. Indeed, we discover that the area of the CS event horizon diverges at late times.

This surprising result leads to a puzzle: if we associate the entropy of the corresponding CFT conformal soliton state to the area of the CS event horizon, as is usually assumed to be the case, then we find that this entropy likewise diverges at late times. But the conformal soliton describes a shear-free flow, with no entropy production whatsoever. Said differently, the conformal transformation from the CFT on $\mathbf{S}^3 \times \mathbf{R}^1$ to the CFT on $\mathbf{R}^{3,1}$ should leave the entropy invariant. But the former describes a perfect fluid in global thermodynamic equilibrium: its entropy is finite and constant in time.

In fact, it has been argued previously in several different contexts [25, 26] that it may be more appropriate to associate the entropy of the CFT configuration to the area of the apparent horizon rather than the event horizon in the bulk dual. We will show that the apparent horizon in this Poincaré slicing still coincides with the global Schwarzschild-AdS event horizon, whose area is indeed constant. Thus, this is a case where the event horizon and the apparent horizon are very different. The CS geometry therefore provides a good testing ground for studying the distinction between the event and apparent horizons and the role they play for the associated CFT dual. We see that in this case the CFT entropy is clearly more naturally associated with the latter rather than the former.

This might also seem enigmatic, as it was argued in [16] that the apparent horizon and the event horizon track each other closely in the hydrodynamic regime. Again, the essential difference between the cases we consider here and [16] is that in that general analysis, it was assumed that the geometry would settle down at late times to a stationary finite-temperature black hole. Neither of the geometries we consider have this property. For the Bjorken flow, we find qualitatively similar results, in that the apparent horizon and event horizon nevertheless track each other closely. But for the conformal soliton, the late time boundary conditions

force the apparent horizon and the event horizon to behave very differently.

In the next section, we consider the Bjorken flow, summarizing previous work and determining the location of the event horizon. In §3, we consider the horizons in the conformal soliton, focusing on the three-dimensional case, where the calculations are simplest. We conclude in §4 with a discussion of the lessons of these examples and open problems for the future. The Appendices collect generalizations and some of the more technical arguments.

2 Boost invariant flow

As described in the Introduction, the Bjorken flow (BF) plays a central role in understanding the post-thermalization evolution of the QGP produced in heavy-ion collisions. The basic physical picture developed in [1] is that in the central rapidity region of ultra-relativistic collisions of heavy ions, assuming local thermal equilibrium, one can model the flow of the plasma via quasi-ideal hydrodynamics. In the hydrodynamic description, it is assumed that the fluid evolution respects the boost symmetry along the collision axis. This implies a boost invariant expansion of the fluid, consistent with the observed distribution of the particles in the collision process.

2.1 Bjorken hydrodynamics

To understand the hydrodynamics in the BF, consider Minkowski spacetime $\mathbf{R}^{3,1}$ written in Milne-type coordinates which respect boost invariance in a $\mathbf{R}^{1,1}$ subspace, i.e.,

$$ds^2 = -d\tau^2 + \tau^2 dy^2 + dx_\perp^2 . \quad (2.1)$$

The coordinates τ and y measure the proper time and rapidity in the longitudinal direction respectively, and x_\perp collectively denotes the transverse directions. For a conformally invariant fluid, the equations of motion of hydrodynamics, viz., energy momentum conservation and tracelessness of stress tensor,

$$\nabla_\mu T^{\mu\nu} = 0 , \quad T_\mu{}^\mu = 0 , \quad (2.2)$$

can be shown to constrain the dynamics to be derivable from a single function $\varepsilon(\tau)$ which is conveniently taken to be the energy density [2]. For an ideal conformal fluid, the equations of motion lead to a power law fall-off for the energy density and temperature

$$\varepsilon(\tau) = \frac{\varepsilon_0}{\tau^4} , \quad T \sim \tau^{-\frac{1}{3}} , \quad (2.3)$$

with the entropy per unit rapidity remaining constant. It is clear from (2.3) that there is a divergent amount of energy density localized on the forward light-cone, $\tau = 0$. Nevertheless,

as the fluid expands the energy density diffuses throughout the forward light-cone. At late times the ideal hydrodynamic description becomes more and more accurate in the interior of the light-cone in $\mathbf{R}^{1,1}$.

One can in fact go beyond the ideal fluid description of the BF and argue that an expansion in powers of $\tau^{-\frac{2}{3}}$ corresponds to the derivative expansion in the fluid dynamics. Recall that the hydrodynamic description can be thought of as an IR effective field theory, valid at long wavelengths, for any interacting system that achieves local thermal equilibrium. Given this, one can explore the dissipative corrections to fluid dynamics by studying the system in a perturbation expansion at large proper time τ . This was carried out in [3] to include viscous corrections. To derive the transport properties of the plasma, the authors examined the gravitational dual of the flow in the context of the AdS/CFT correspondence.

2.2 The gravity dual to Bjorken flow

In [2, 3], the authors also constructed the bulk geometry dual to the given fluid dynamical evolution using the AdS/CFT correspondence.⁴ The bulk metric was written in a Fefferman-Graham type coordinate chart, and Einstein's equations were solved to the desired order in a power series in $\tau^{-2/3}$ at late times. To be precise, consider an ansatz for the spacetime metric:

$$ds^2 = \frac{1}{z^2} \left(-e^{\alpha(\tau,z)} d\tau^2 + \tau^2 e^{\beta(\tau,z)} dy^2 + e^{\gamma(\tau,z)} dx_{\perp}^2 \right) + \frac{dz^2}{z^2} . \quad (2.4)$$

The Fefferman-Graham expansion involves solving Einstein's equations for the functions α , β and γ perturbatively in the region $z \ll 1$, subject to asymptotic AdS boundary conditions, i.e., one expands the functions as⁵

$$\alpha(\tau, z) = \sum_{n=0} \alpha_n(\tau) z^{4+2n} , \quad (2.5)$$

and similarly for β and γ . This perturbatively constructed solution, it was argued, could be re-expressed in terms of a scaling variable

$$v = \frac{z}{\tau^{\frac{1}{3}}} , \quad (2.6)$$

which then allows one to work at late proper times $\tau \gg 1$. This analysis leads to the above mentioned perturbation expansion in $\tau^{-2/3}$. For details we refer the reader to [2].

⁴The gravity dual to Bjorken flow in 1+1 dimensions was discussed in [27]. Note that there isn't a hydrodynamic limit in 1+1 dimensions for conformal fluids. This is reflected in the bulk by the solutions being just the BTZ black hole written in a different coordinate chart. In [28] the dual spacetime to a spherically symmetric boost invariant flow was constructed

⁵Recall that in the Fefferman-Graham coordinates used in (2.4) the boundary of the spacetime is at $z = 0$. We have also for brevity ignored $\log z$ terms which appear in even spacetime dimensions.

By demanding that the spacetime thus constructed be regular, it was shown that the shear-viscosity of the plasma saturates the universal lower bound $\eta/s = 1/4\pi$. To demand regularity, the authors looked at the first non-trivial curvature invariant, the Kretschmann scalar, $R_{\mu\nu\rho\sigma} R^{\mu\nu\rho\sigma}$, expanded in a power series in $\tau^{-2/3}$. Of course, well behavedness of a single curvature invariant by itself does not guarantee that the spacetime is completely regular, but this was sufficient to fix the transport coefficients.

In [18, 20] this geometry was examined at higher orders, and it was found that the spacetime appears to be singular (at the third order). The appearance of this singularity would seem contrary to the general analysis of the fluid-gravity correspondence in [5], where black hole solutions dual to arbitrary fluid flows in the boundary field theory were constructed in a derivative expansion and conjectured to be regular. However, the BF spacetime does not settle down to a stationary finite-temperature black hole, so the demonstration of the existence of a regular event horizon in [16] does not apply in this case.

In fact, the appearance of a singularity is associated with a poor choice of coordinate system: in [2, 3] the authors chose to work with the Fefferman-Graham coordinatization of AdS, which was argued in [16, 10] to be problematic for discussing regularity issues. Indeed, to avoid this subtlety, the original construction of gravitational duals of fluid flows was done in ingoing Eddington-Finkelstein type coordinates in [5]. In [21, 22] (see also [23]) the gravity dual to the BF was constructed in the Eddington-Finkelstein coordinates, and it was argued that in these coordinates the BF geometry is indeed regular.

Let us review the details of this construction: we will follow the conventions of [22] (except for using τ rather than τ_+ to denote the proper time coordinate). As we want the bulk geometry to asymptote to (2.1) on the boundary and naturally adapt the coordinate chart to ingoing null geodesics, we have a metric ansatz:

$$ds^2 = -r^2 a d\tau^2 + 2 d\tau dr + r^2 \tau^2 e^{2(b-c)} \left(1 + \frac{1}{u \tau^{2/3}} \right)^2 dy^2 + r^2 e^c dx_{\perp}^2, \quad (2.7)$$

where

$$u \equiv r \tau^{1/3}, \quad (2.8)$$

and the functions a , b , c depend on u and r .

The idea is to use (2.7) as an ansatz and solve Einstein's equations iteratively in a late time expansion, $\tau \rightarrow \infty$, keeping u fixed. In order to do so, one assumes that the functions a , b and c can be expanded as

$$\begin{aligned} a(\tau, u) &= a_0(u) + a_1(u) \tau^{-2/3} + a_2(u) \tau^{-4/3} + a_3(u) \tau^{-2} + \mathcal{O}(\tau^{-8/3}), \\ b(\tau, u) &= b_0(u) + b_1(u) \tau^{-2/3} + b_2(u) \tau^{-4/3} + b_3(u) \tau^{-2} + \mathcal{O}(\tau^{-8/3}), \\ c(\tau, u) &= c_0(u) + c_1(u) \tau^{-2/3} + c_2(u) \tau^{-4/3} + c_3(u) \tau^{-2} + \mathcal{O}(\tau^{-8/3}). \end{aligned} \quad (2.9)$$

To solve the Einstein equations, one imposes the boundary conditions,

$$a|_{u=\infty} = 1, \quad b|_{u=\infty} = 0, \quad c|_{u=\infty} = 0, \quad (2.10)$$

which ensure that the spacetime has boundary metric consistent with the Bjorken flow, (2.1). We will denote the metric obtained by this procedure at order $\mathcal{O}(\tau^{-2k/3})$ as $g^{(k)}$, so that $g^{(k)}$ is specified completely by the functions $a_i(u)$, $b_i(u)$ and $c_i(u)$ for $i \leq k$.

The Einstein's equations for gravity (with a negative cosmological constant) were solved order by order in the late time expansion, and the solutions depend only on a set of arbitrary constants. These constants can be fully determined order by order by requiring that the geometry be asymptotically AdS and that the Kretschmann scalar is regular except at the origin $r = 0$ [21, 22]. This determines the choice of transport coefficients along the lines of the original philosophy espoused in [3]. This is different from the result of [18, 20] because working in Eddington-Finkelstein coordinates imposes regularity on the future event horizon in the bulk geometry, which is the physically correct condition. We should note however that the regularity of a particular curvature invariant is a necessary but not a sufficient condition for regularity.

The rationale for the use of the Eddington–Finkelstein coordinates was given originally in [5] (see also [10]). To motivate this consider the hydrodynamic description of any interacting field theory; as explained earlier this makes sense so long as one achieves local thermal equilibrium. In the AdS/CFT context one expects each locally equilibrated domain in the field theory to have as gravity dual a stationary black hole solution. These domains in the field theory extend into the bulk as “tubes” along ingoing null geodesics. In a sense, the construction of the gravity solution perturbatively in boundary derivatives corresponds to patching together these tubes (after all, this is what hydrodynamics achieves in the boundary description). Specifically, the tubes of relevance were argued to be centered along radially ingoing null geodesics, which in the coordinatization of [5, 16] are just $x^\mu = \text{constant}$ with x^μ being the boundary coordinates. In the present case of the Bjorken flow, the Eddington-Finkelstein coordinates not only makes issues of regularity more transparent, but also provides a sensible coordinate chart to perform the late proper time expansion. Since there is no pathology in the coordinate chart in the zeroth order solution (the metric being completely regular there), it can then be shown that the higher order corrections in the late proper time expansion remain regular [21, 22].⁶

At zeroth order, one obtains the spacetime with metric $g^{(0)}$:

$$ds^2 = -r^2 \left(1 - \frac{w^4}{u^4}\right) d\tau^2 + 2 d\tau dr + r^2 \tau^2 \left(1 + \frac{1}{u \tau^{2/3}}\right) dy^2 + r^2 dx_\perp^2, \quad (2.11)$$

where w is a constant, whose precise value will not play a role in our discussion. This metric is consistent with the original derivation given in [2]. Note that this metric reduces to pure AdS space for $w \rightarrow 0$. Naively it appears that (2.11) is a black hole metric with the location

⁶ Essentially the distinction between the use of Fefferman-Graham and the Eddington-Finkelstein coordinates may be traced to the trustworthiness of the late proper time expansion of various curvature invariants.

of the horizon being given by the zero locus of $g_{\tau\tau}^{(0)}$, i.e.,

$$r(\tau) = \frac{w}{\tau^{\frac{1}{3}}} . \quad (2.12)$$

For the metrics at higher orders, and a comprehensive discussion of the derivation, we refer the reader to [22].

2.3 Apparent horizon for the BF spacetime

To further bolster the claim that the spacetime dual to the BF (2.7) is regular, in [22] the apparent horizon of the spacetime was determined explicitly up to second order in the τ expansion. The presence of an apparent horizon implies by virtue of the singularity theorems that the spacetime will evolve into a singularity in the future. The idea of [22] was to argue that this apparent horizon must be enclosed by a global event horizon, concealing the singularities from the asymptotic region. This is a plausible argument, but to make it rigorous we would need to check that the spacetime asymptopia is complete.⁷ This requires a better understanding of the global structure, which is the main focus of the present work. We will explicitly construct the event horizon in this geometry in the next section, and demonstrate that the spacetime is regular on and outside the event horizon. Before turning to that however, it will be useful to review the construction of the apparent horizon in [22].

The apparent horizon is given by the null hypersurface for which the expansion of the outgoing null geodesics vanishes. For the metric (2.7), the vectors tangent to the ingoing and outgoing radial null geodesics are given by

$$l_-^a = - \left(\frac{\partial}{\partial r} \right)^a , \quad l_+^a = \left(\frac{\partial}{\partial \tau} \right)^a + \frac{r^2 a}{2} \left(\frac{\partial}{\partial r} \right)^a , \quad (2.13)$$

up to some overall normalisation factors that are irrelevant for this calculation. Note that we are considering congruences that emanate normal to the co-dimension two spacelike surface in the spacetime and are exploiting the symmetries of the geometry to restrict our attention to normals pointing in the radial direction. Then the expansions θ_{\pm} are defined as

$$\theta_{\pm} = \mathcal{L}_{\pm} \ln \mu , \quad (2.14)$$

where \mathcal{L}_{\pm} denotes the Lie derivative along l_{\pm}^a and μ is the volume of the null hypersurface,⁸

$$\mu = r^3 \tau e^b \left(1 + \frac{1}{\tau r} \right) . \quad (2.15)$$

⁷Showing that the event horizon is outside the apparent horizon also requires that appropriate energy conditions are satisfied. Since the full geometry solves the vacuum Einstein equations with a cosmological constant, the null energy condition is of course satisfied. As we'll see below, however, if we work order by order in perturbation theory, at low orders the energy conditions are not be satisfied.

⁸This exploits crucially the fact that the vectors $\left(\frac{\partial}{\partial y} \right)^a$ and $\left(\frac{\partial}{\partial x_{\perp}} \right)^a$ are Killing in the geometry (2.7).

The quantity $\Theta = \theta_+ \theta_-$ is an invariant,⁹ and hence the location of the apparent horizon can be found by solving

$$\Theta = 0 \tag{2.16}$$

for $r(\tau)$. Since the geometry is only known in a perturbative expansion in τ for large proper time, the location of the apparent horizon will also be determined in the power series. Writing

$$r_A(\tau) = r_{A0} \tau^{-\frac{1}{3}} + r_{A1} \tau^{-1} + r_{A2} \tau^{-\frac{5}{3}} + \mathcal{O}\left(\tau^{-\frac{7}{3}}\right), \tag{2.17}$$

substituting this expansion into (2.16), and using the previously determined functions a and b , we can find $r(\tau)$ order by order in $\tau^{-2/3}$. In [22] this procedure was carried out up to the second order for the metric $g^{(2)}$, with the result:¹⁰

$$r_{A0}^{(2)} = w, \quad r_{A1}^{(2)} = -\frac{1}{2}, \quad r_{A2}^{(2)} = \frac{8 + 3\pi - 4 \ln 2}{72w}. \tag{2.18}$$

It is not surprising that the zeroth order location of the apparent horizon coincides with the naive horizon (2.12).

2.4 Event horizon for the BF spacetime

As discussed earlier, to convincingly demonstrate the regularity of the spacetime (2.7), we have to show that the spacetime has a well behaved global event horizon. This is defined as the boundary of the past of future infinity \mathcal{I}^+ . It is by definition a null surface and furthermore since it is the boundary of a causal set, is generated by null geodesics. In the cases where the solution settles down to a stationary configuration asymptotically, we know the position of the horizon at late times, and can evolve back using the geodesic equation to determine the location of the event horizon. In the present case however, (2.7) does not appear to settle down to a known stationary configuration. We will therefore determine the location of the horizon directly, by studying the geodesic motion on the spacetime (2.7) and determining which points cannot send signals to infinity. The analysis is simplified by the fact that (2.7) is co-homogeneity two, so the problem reduces to studying geodesic motion in the (r, τ) plane.

Since one has three Killing fields $\left(\frac{\partial}{\partial y}\right)^a$ and $\left(\frac{\partial}{\partial x_\perp}\right)^a$ the location of the horizon is simply given by a curve $r(\tau)$. The null geodesic equation reduces to

$$\frac{d}{d\tau} r(\tau) = \frac{1}{2} r(\tau)^2 a(r(\tau), \tau). \tag{2.19}$$

⁹More precisely, it is invariant under reparametrisations of the scalars that define the null hypersurface.

¹⁰In what follows use the notation $r_{Ai}^{(k)}$ and $r_{Ei}^{(k)}$ to denote the coefficients in the expansion of the apparent and event horizon for the metric $g^{(k)}$.

The event horizon is the outermost solution of this equation which does not reach $r = \infty$ at finite τ . At late times, $r(\tau)$ for the event horizon can be shown to admit an expansion in $\tau^{-2/3}$ of the form

$$r_E(\tau) = r_{E0} \tau^{-1/3} + r_{E1} \tau^{-1} + r_{E2} \tau^{-5/3} + \mathcal{O}(\tau^{-7/3}), \quad (2.20)$$

where the r_{Ei} 's are some yet to be determined constants. These constants can be found by solving (2.19) order by order using the previously determined expansion for $a(\tau, u)$ at the same order. Using the metric $g^{(2)}$ quoted in [22] we find that

$$r_{E0}^{(2)} = w, \quad r_{E1}^{(2)} = -\frac{1}{2}, \quad r_{E2}^{(2)} = \frac{12 + 3\pi - 4 \ln 2}{72w}, \quad (2.21)$$

This gives the location of the event horizon up to second order in the late time expansion.

Comparing, (2.21) with (2.18), we see that the event horizon indeed lies outside the apparent horizon at this order. Furthermore, the spacetime metric (2.7) is regular on and outside the event horizon: the singularity at $r = 0$ is cloaked by the event horizon. We have thus demonstrated that the spacetime at second order in the perturbation expansion, with metric $g^{(2)}$, is indeed regular.

A curiosity at leading order: The location of the event horizon differs from the location of the apparent horizon derived in [22] at second order in the expansion in $\tau^{-2/3}$. Of course, we need to work with the second order metric $g^{(2)}$ to study the position of the horizon to this order. However, it is worth remarking on a curious behaviour which is seen if we work with the metric at the zeroth order, and ask about the difference between the locations of the apparent and event horizons.

It is clear that we should trust the coefficient r_k in the expansion for the location of the apparent/event horizon in (2.17), (2.20) only upon using the metric $g^{(k)}$. This is because the metric $g^{(k)}$ only satisfies Einstein's equations to $\mathcal{O}(\tau^{-2k/3})$. If we consider the metric $g^{(0)}$, we can thus only trust r_{A0} and r_{E0} in the expansions for the apparent horizon, (2.18), and the event horizon, (2.21). The event and apparent horizons lie on top of each other at this order. Nevertheless, given the metric at some order we can ignore the fact that it doesn't satisfy the appropriate field equations and treat the residue as some effective energy-momentum tensor required to support the geometry. One can then study the metric at any given order as a spacetime in its own right and ask for the locations of the apparent and event horizons at higher orders in the τ expansion. For $g^{(0)}$ we find

$$\begin{aligned} r_{A0}^{(0)} &= w, & r_{A1}^{(0)} &= -\frac{1}{6}, & r_{A2}^{(0)} &= \frac{11}{12w}, \\ r_{E0}^{(0)} &= w, & r_{E1}^{(0)} &= -\frac{1}{6}, & r_{E2}^{(0)} &= \frac{7}{72w}. \end{aligned} \quad (2.22)$$

We see that the apparent horizon for the artificial metric $g^{(0)}$ lies outside the event horizon! This contradicts the expected behaviour (seen in $g^{(2)}$) that the apparent horizon should lie

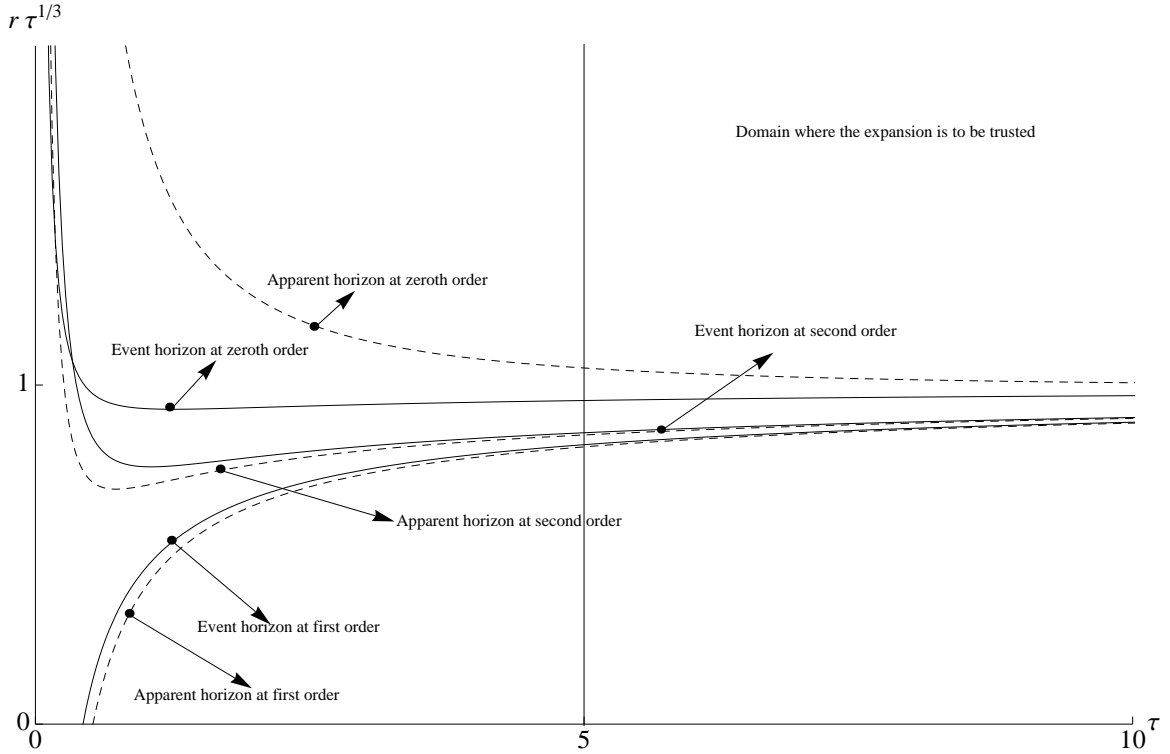


Fig. 1: Illustration of the horizons for the Bjorken flow metrics $g^{(k)}$ at various orders in the perturbation expansion. The event horizons are the solid curves while the apparent horizons are the dashed curves. The locations of the horizons of course should only be trusted at late times as indicated in the figure.

behind the event horizon. We illustrate the location of the horizons at various orders in Fig. 1.

The explanation for the apparent horizon lying outside the event horizon is simple: the geometry $g^{(0)}$ fails to be a solution of the vacuum equations beyond the leading order in perturbation theory, and the required stress tensor source violates the energy conditions. This can be checked by computing $T_{\mu\nu}^{\text{bulk}} = R_{\mu\nu} - \frac{1}{2} R g_{\mu\nu} - 6 g_{\mu\nu}$ and seeing that the null energy condition is violated for (2.11).

We have thus seen that the BF geometry is a regular black hole spacetime. Despite the dual fluid flow not quite settling down at late times as required for the analysis of [16], the spacetime event horizon can nevertheless be inferred by appropriate ray tracing.

3 The Conformal Soliton flow

In this section we will consider the conformal soliton (CS) geometry discussed initially in [24] as our second example of a dynamical flow. The CS spacetime is extremely simple – it is just the global AdS black hole sliced in Poincaré coordinates.

As explained in §1, to obtain the CS_{d+1} spacetime we take the global Schwarzschild- AdS_{d+1} black hole, which is dual to a fluid in global thermal equilibrium in the Einstein Static Universe $\mathbf{S}^{d-1} \times \mathbf{R}^1$, and consider it in a ‘Poincaré patch’. From the dual field theory point of view, we are making a conformal transformation to map the field theory on $\mathbf{S}^{d-1} \times \mathbf{R}^1$ to the field theory on Minkowski space, $\mathbf{R}^{d-1,1}$. This maps the stationary fluid on the Einstein Static Universe to a time-dependent fluid configuration on Minkowski space. From the bulk spacetime point of view, this corresponds to considering only the portion of the null infinity \mathcal{I}^+ of global Schwarzschild- AdS_{d+1} restricted to this Minkowski patch in the Einstein Static Universe; we call this subregion on the boundary \mathcal{I}_{CS}^+ . The corresponding Poincaré patch in the bulk contains not only the region outside the black hole which is simply the portion of global Schwarzschild- AdS_{d+1} visible from this portion of null infinity, but also a finite region inside the black hole. The former is bounded by past and future Poincaré horizons, as in the description of global AdS in Poincaré coordinates, whereas the latter covers a larger region, whose boundary we’ll refer to as “Poincare edge”.

We will be interested in the global structure of the solution and will find the event horizon in §3.2 and the apparent horizon in §3.4. For simplicity, we will consider the situation in 2+1 dimensions, i.e., concentrate on the BTZ black hole. This lower dimension example captures all of the essential features of the calculation and has the significant advantage of being algebraically simpler. We will comment on the extension to higher dimensions in Appendix A. Also, without loss of generality we will set the AdS radius to unity, which translates to measuring all lengths in AdS units.

3.1 The BTZ spacetime as a conformal soliton

We follow [24] and describe a region in the bulk geometry of the Schwarzschild- AdS_{d+1} spacetime in Poincaré coordinates, applying a specific coordinate transformation, one that transforms global AdS_{d+1} into Poincaré AdS, to the black hole spacetime.

The coordinate transformation between the global coordinates $\{\tau, r, \phi\}$ in which pure AdS_3 has metric

$$ds^2 = -(r^2 + 1) d\tau^2 + \frac{dr^2}{r^2 + 1} + r^2 d\phi^2 \quad (3.1)$$

and the Poincaré coordinates $\{t, z, x\}$ in which the metric is

$$ds^2 = \frac{-dt^2 + dz^2 + dx^2}{z^2} \quad (3.2)$$

can be written as¹¹

$$z = \frac{1}{\sqrt{r^2 + 1} \cos \tau + r \cos \phi}, \quad t = \frac{\sqrt{r^2 + 1} \sin \tau}{\sqrt{r^2 + 1} \cos \tau + r \cos \phi}, \quad x = \frac{r \sin \phi}{\sqrt{r^2 + 1} \cos \tau + r \cos \phi}. \quad (3.3)$$

When this transformation is applied to pure AdS spacetime, the Poincaré edge at $z = \infty$ actually coincides with the Poincaré horizon, which is the null surface bounding the causal wedge of \mathcal{I}_{CS} . In the global coordinates, this surface is given by the relation $\sqrt{r^2 + 1} \cos \tau + r \cos \phi = 0$. Note that this relation describes the Poincaré edge if we apply the coordinate transformation (3.3) to a more general asymptotically-AdS spacetime as well; but in the general case this Poincaré edge no longer coincides with the null Poincaré horizon.

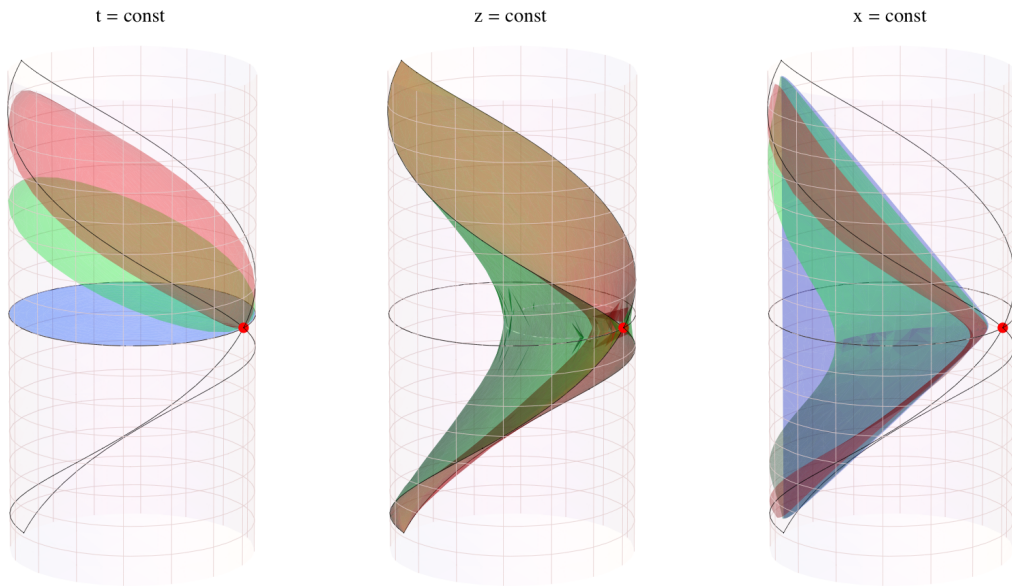


Fig. 2: Illustration of Poincaré coordinates superposed on conformally compactified AdS. The surfaces $t = 0, 1, 5$ (left), $z = 1, 5$ (middle), and $x = 0, 1, 5$ (right) are plotted, with colour-coding blue for 0, green for 1, and red for 5. To guide the eye, superposed are also the boundary of the \mathcal{I}_{CS}^+ corresponding to $t = \pm\infty$ and the $t = 0$ boundary slice (black curves).

Fig. 2 gives a plot of the constant Poincaré coordinates in the AdS spacetime. The constant Poincaré time t surfaces (left plot) are all pinned at the red reference point i_{CS}^0 (which in global coordinates corresponds to $\tau = 0, \phi = \pi$, and $r = \infty$), with the $t = \pm\infty$

¹¹This transformation can be easily obtained by writing (3.1) and (3.2) in terms of embedding coordinates describing a hyperboloid in $\mathbf{R}^{2,2}$. Note, however, that this is not the only coordinate transformation which implements the desired conformal transformation on the boundary; in fact, it is not even the simplest one. In Appendix C we use an algebraically simpler transformation, which has the same limiting relations on the boundary $r \rightarrow \infty$.

surfaces coinciding with the Poincaré edge. The constant z surfaces (middle plot) interpolate from the \mathcal{S}_{CS}^+ at $z = 0$ to the Poincaré edge at $z = \infty$, with the surfaces having round cross-sections at $t = 0$ slice, tangent to i_{CS}^0 . Finally, the constant x slices (right plot) are pinned at i_{CS}^0 , and interpolate from a section of $\phi = 0, \pi$ plane at $x = 0$ to half of the Poincaré edge at $x = \pm\infty$.

Now, consider the BTZ spacetime with metric

$$ds^2 = -(r^2 - r_+^2) d\tau^2 + \frac{dr^2}{r^2 - r_+^2} + r^2 d\phi^2 \quad (3.4)$$

and perform the coordinate transformation (3.3) to obtain the metric in Poincaré coordinates. The resulting geometry is what we call the CS spacetime. We do not give the form of the bulk geometry in these coordinates explicitly, as even in the simple BTZ case it is rather messy and unilluminating, but it is clear that the metric will appear time-dependent in these coordinates.¹²

As required, the coordinate transformation (3.3) corresponds to a conformal transformation on the boundary of the AdS spacetime. It maps the Einstein Static Universe to Minkowski space. The conformal transformation can be inferred by restricting the transformation (3.3) to the boundary ($r \rightarrow \infty$), where it results in the map:

$$t = \frac{\sin \tau}{\cos \tau + \cos \phi}, \quad x = \frac{\sin \phi}{\cos \tau + \cos \phi}. \quad (3.5)$$

It is easy to check that (3.5) maps the Lorentzian cylinder $\mathbf{S}^1 \times \mathbf{R}^1$ to $\mathbf{R}^{1,1}$,

$$ds^2 = -dt^2 + dx^2 = W^2 (-d\tau^2 + d\phi^2), \quad (3.6)$$

with

$$W = \frac{1}{\cos \tau + \cos \phi} = \frac{1}{2} \sqrt{4t^2 + (1 + r^2 - t^2)^2} \quad (3.7)$$

In the dual CFT description, the global Schwarzschild-AdS black hole corresponds to a static ideal fluid in thermal equilibrium. The field theory stress tensor transforms homogeneously under conformal transformations [29], so applying the conformal transformation (3.5) will give a time-dependent fluid in Minkowski space, but one which still describes an ideal fluid. That is, this time-dependent fluid flow is free of dissipation. We give a brief review of the fluid description in Appendix B and refer the reader to [24] for a comprehensive discussion in the AdS₅ case.

3.2 Event horizon for the CS spacetime

Since we are restricting consideration to a subregion \mathcal{S}_{CS}^+ of the full future null infinity \mathcal{S}^+ of the global Schwarzschild-AdS spacetime, the event horizon of the CS spacetime will be

¹²In fact, given that the coordinate transformation (3.3) involves all three coordinates, the resulting metric in the Poincaré coordinates has no manifest symmetries.

different from the event horizon in global Schwarzschild-AdS. This event horizon will constitute the boundary of the region of spacetime visible from \mathcal{I}_{CS}^+ , so it is the proper analogue of the Poincaré horizon in pure AdS. Intuitively, we expect it to interpolate smoothly between the black hole horizon $r = r_+$ at very early times and the surface $z = \infty$ close to the boundary, corresponding to our naive picture of the CS spacetime as describing a black hole falling across the Poincaré horizon.

A-priori, one might worry that from a gravitational viewpoint, consideration of \mathcal{I}_{CS}^+ seems rather ad hoc, since we are by fiat restricting to a subset of the maximally extended spacetime's \mathcal{I}^+ . However, this is well-justified by the field theory. In the AdS/CFT correspondence one prescribes a conformal structure for the boundary. Then a given boundary metric corresponds to a particular representative and one studies field theory on a background manifold with this prescribed metric. However, one is free to change the background on which the field theory lives. For the field theory on the Einstein Static Universe, one considers the global spacetime, whereas for the field theory on Minkowski space we are required to restrict attention to the Poincaré patch. For an observer in this boundary Minkowski space we have to define the horizon using \mathcal{I}_{CS}^+ . Our construction can be thought of as an observer dependent horizon in the spacetime, with the Minkowski observer being singled out by field theoretic considerations.

We could construct this horizon by working with the CS geometry in the Poincaré coordinates, and finding the null surface with the requisite late time behaviour, analogously to §2.4. However, this is rather impractical. Instead, we can work with the metric (3.4) in the global coordinates, and look for the surface which bounds the past of \mathcal{I}_{CS}^+ . In BTZ coordinates, we can take \mathcal{I}_{CS}^+ to be the connected region at $r = \infty$ containing $\tau = 0$ with $\cos \tau + \cos \phi \geq 0$. The CS event horizon is then the boundary of the causal past of this region. Since all points in \mathcal{I}_{CS}^+ lie in the causal past of the boundary point $(r = \infty, \tau = \pi, \phi = 0)$, the problem of finding the CS event horizon reduces to the problem of finding null geodesics ending on this point.

Finding such null geodesics in (3.4) is a straightforward exercise. The main subtlety arises from the fact that the null geodesics ending on this boundary point caustic, so they do not form a smooth surface. Indeed, the presence of caustic points is typical for an event horizon in a generic dynamical spacetime; here the caustic locus is actually very simple, occurring only at $\phi = \pi$ (which is identified with $\phi = -\pi$). A caustic at $\phi = \pi$ is expected from the symmetry under $\phi \rightarrow -\phi$. It is easy to show that the event horizon is smooth for $\phi \neq \pm\pi$. We now proceed to determine this event horizon explicitly.

The geodesic equations are

$$\dot{r}^2 = 1 - \ell^2 + \frac{\ell^2 r_+^2}{r^2}, \quad \dot{\tau} = \frac{1}{r^2 - r_+^2}, \quad \dot{\phi} = \frac{\ell}{r^2}, \quad (3.8)$$

where $\dot{} = \frac{d}{d\lambda}$ with λ being the affine parameter along the geodesic and ℓ is the conserved quantity along each geodesic corresponding to angular momentum per energy. We can think

of ℓ as specifying which geodesic we take and λ as the position along that geodesic. Equations (3.8) can be immediately integrated to give

$$\begin{aligned} r(\lambda, \ell)^2 &= (1 - \ell^2) \lambda^2 - \frac{\ell^2 r_+^2}{1 - \ell^2}, \\ \tau(\lambda, \ell) &= \pi - \frac{1}{r_+} \operatorname{arccoth} \left(\frac{1 - \ell^2}{r_+} \lambda \right), \\ \phi(\lambda, \ell) &= -\frac{1}{r_+} \operatorname{arccoth} \left(\frac{1 - \ell^2}{\ell r_+} \lambda \right), \end{aligned} \quad (3.9)$$

where we have chosen the constants of integration so that the geodesics have a future endpoint at $(r = \infty, \tau = \pi, \phi = 0)$. The relations (3.9) describe a 2-surface parameterized by λ and ℓ with $0 \leq \ell < 1$ and $\lambda_{\min}(\ell) \leq \lambda < \infty$. This 2-surface corresponds to the CS event horizon. Note that the geodesics with $\tanh(r_+ \pi) < \ell < 1$ terminate on the line of caustics at $\phi = \pi$, and λ_{\min} is determined by cutting off the surface when the geodesics caustic. The caustic locus is obtained by solving $\phi(\lambda, \ell) = \pi$, giving

$$r_c(\ell) = -\frac{\ell}{\sqrt{1 - \ell^2}} \frac{r_+}{\sinh(\pi r_+)}, \quad \tau_c(\ell) = \pi - \frac{1}{r_+} \operatorname{arccoth}(\ell \coth(\pi r_+)). \quad (3.10)$$

This generates the curve of caustics, described by a relation between τ and r , with $\phi = \pi$, given by

$$\tau_c(r) = \pi - \frac{1}{r_+} \operatorname{arctanh} \left(\frac{\sqrt{r^2 \sinh^2(\pi r_+) + r_+^2}}{r \cosh(\pi r_+)} \right). \quad (3.11)$$

One important detail to note here is that the curve of caustics starts to exist only for ℓ larger than some minimum value ℓ_{\min} , where¹³ $\tau \rightarrow -\infty$. In particular,

$$\ell_{\min} = \tanh(\pi r_+), \quad (3.12)$$

and $r_c(\ell_{\min}) = r_+$. For large BTZ black holes $r_+ > 1$, ℓ_{\min} gets exponentially close to unity.

Instead of parameterising the horizon by λ and ℓ as in (3.9), it is in practice a bit simpler, though physically equivalent, to use the fact that $r(\lambda)$ is a monotonic function, and think of the event horizon as a surface parameterised by r and ℓ :

$$\begin{aligned} \tau(r, \ell) &= \pi - \frac{1}{r_+} \operatorname{arccoth} \left(\frac{\sqrt{(1 - \ell^2) r^2 + \ell^2 r_+^2}}{r_+} \right), \\ \phi(r, \ell) &= -\frac{1}{r_+} \operatorname{arcsinh} \left(\frac{\ell r_+}{\sqrt{1 - \ell^2}} \frac{1}{r} \right). \end{aligned} \quad (3.13)$$

¹³ Note that in order to stay within the CS spacetime (in particular to the future of the past Poincaré edge), we need a stronger constraint: rather than bounding ℓ by $\tau \rightarrow -\infty$, we will bound ℓ by $t \rightarrow -\infty$, which provides a more stringent bound.

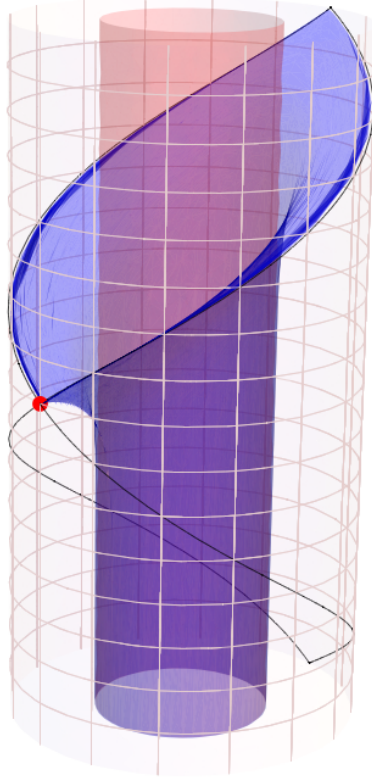


Fig. 3: Plot of the event horizon of the CS spacetime. For ease of visualization we have also plotted the location of the event horizon of the global Schwarzschild-AdS black hole.

It is easy to confirm that the surface described by (3.9) or (3.13) is indeed a null surface. For instance, the induced metric on this 2-surface is simply

$$ds_{ind}^2 = \frac{d\ell^2}{(1 - \ell^2)^2}, \quad (3.14)$$

which is clearly degenerate, as required of the event horizon.

Fig. 3 shows a plot of the event horizon. As apparent from the plot, the CS event horizon lies outside the global event horizon at r_+ . Indeed, at late Poincaré times, the event horizon approaches the intersection of the global spacetime boundary \mathcal{I}^+ with the Poincaré horizon.

3.3 Event horizon area & field theory entropy

One of the most important and physically interesting attributes of the event horizon is the area of its cross-sections, which we would usually take to give the entropy of the corresponding field theory state. We have seen that the horizon is dynamical, so we expect the area to

be varying. Although the induced metric on the horizon (3.14) does not show explicit time dependence, the area variation arises because of the caustics; if a cross-section of the horizon intersects the line of caustics, it will be parametrized by ℓ lying in some range $0 \leq \ell \leq \ell_{\max}$, where ℓ_{\max} is determined by the intersection of the cross-section with the caustic line. Since the induced metric on the cross-section is given by (3.14), it will then have area

$$\mathcal{A} = 2 \int_0^{\ell_{\max}} \frac{d\ell}{1 - \ell^2} = 2 \operatorname{arctanh} \ell_{\max}. \quad (3.15)$$

Note that $\ell_{\max} > \tanh(r_+\pi)$, so $\mathcal{A} > 2\pi r_+$, that is, the area of the dynamical event horizon on the CS spacetime is always greater than the area of the static horizon in the global BTZ spacetime, as we would expect.

A simple family of cross-sections to consider in the global coordinates is the intersection with surfaces of constant r . From (3.10), we see that for these cross-sections ℓ_{\max} is given by

$$\ell_{\max} = \frac{r \sinh(\pi r_+)}{\sqrt{r_+^2 + r^2 \sinh^2(\pi r_+)}} \quad (3.16)$$

so the area is

$$\mathcal{A} = 2 \operatorname{arctanh} \left(\frac{r \sinh(\pi r_+)}{\sqrt{r_+^2 + r^2 \sinh^2(\pi r_+)}} \right), \quad (3.17)$$

which grows logarithmically at large r .

To translate the variation of the area into a statement of the boundary field theory entropy, we could consider pulling back the area element of the spatial sections of the horizon along radially ingoing null geodesics, as advocated in [16]. This would relate the cross-sections at constant r to some set of spacelike slices in the field theory on Minkowski space. However, it seems more natural to look at slices of constant Poincaré time t , as this is the natural time coordinate from the field theory point of view. We would therefore like to check that the area of cross-sections of constant Poincaré time exhibits a similar behaviour.

We have parameterized the event horizon by $\tau(r, \ell)$ and $\phi(r, \ell)$ in (3.13). In addition the slices of constant Poincaré time are given explicitly in the second equation of (3.3). These three relations can be solved to find the desired cross-sections of the horizon. In particular, along the line of caustics, the Poincaré time is given by

$$t_c(\ell) = \frac{\sqrt{r_c^2(\ell) + 1} \sin \tau_c(\ell)}{\sqrt{r_c^2(\ell) + 1} \cos \tau_c(\ell) - r_c(\ell)}, \quad (3.18)$$

where $r_c(\ell)$ and $\tau_c(\ell)$ are given in (3.10). We can then determine ℓ_{\max} on a cross-section of the horizon at constant Poincaré time by choosing t_c and solving this equation for ℓ . Since it is a complicated transcendental expression, it will not be possible to solve it analytically.

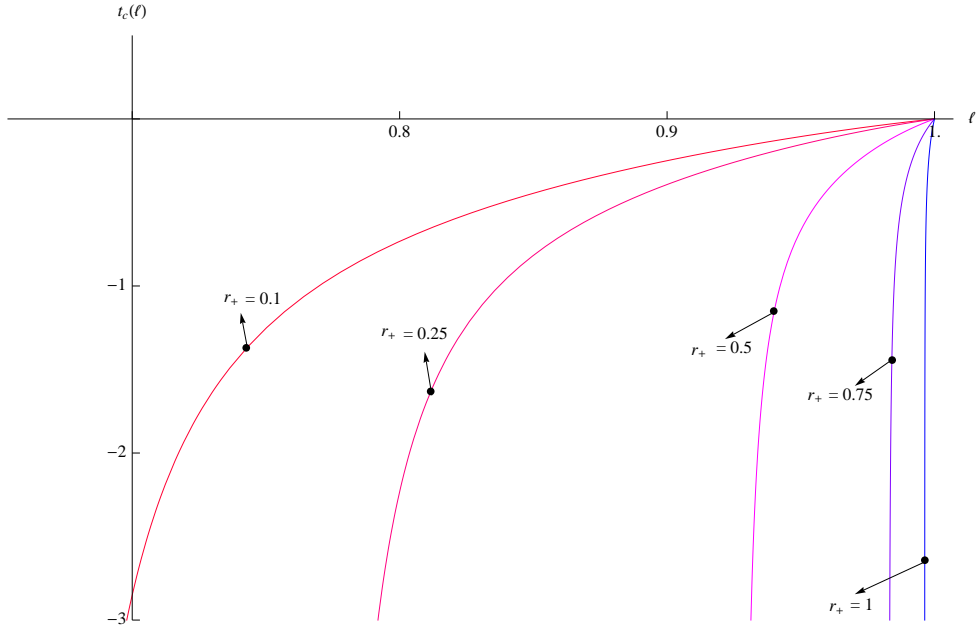


Fig. 4: Behaviour of the Poincaré time along the line of caustics $t_c(\ell)$. We have plotted here the situation for a sampling of BTZ horizon size. As explained in the text, as $r_+ > 1$ (recall that we normalize $L_{\text{AdS}} = 1$) the allowed domain in ℓ shrinks exponentially.

However, we can make some general remarks. The slices $t = 0$ in Poincaré coordinates and $\tau = 0$ in global coordinates coincide. Hence, the $t = 0$ cross-section of the horizon is the same as the $\tau = 0$ cross-section, and hence has $\ell_{\text{max}} = 1$. Further, the slices of $t > 0$ (< 0) lie entirely in the region $\tau > 0$ (< 0) in the global coordinates, while the curve of caustics lies only in the region $\tau < 0$. Hence for any slice with $t \geq 0$, $\ell_{\text{max}} = 1$. All of these slices hence have the same logarithmically divergent area. For the slices with $t < 0$, the area increases monotonically, diverging as $t \rightarrow 0$. Thus, in this slicing as well, we see a logarithmic divergence of the area; the potentially surprising feature is that this divergence occurs at $t = 0$ in this slicing.¹⁴

Furthermore, ℓ_{max} is constrained to be greater than ℓ_{min} determined earlier in (3.12). This is because the Poincaré slice extends only down to $t \rightarrow -\infty$ (the past Poincaré edge) and not all the way down to $\tau = -\infty$. In particular, this implies that even for $t < 0$ the area of the CS event horizon, whilst finite, is nevertheless larger than the area of the event horizon for the global Schwarzschild-AdS black hole.

¹⁴ Although this observation appears to imply that $t = 0$ is special, which is rather surprising given that the CFT state evolves smoothly through $t = 0$, this is really an artifact of our slicing (3.3). Albeit natural, the constant t slices of (3.3) are by no means unique; had we picked the bulk slice anchored at $t = 0$ on the boundary to pass through negative τ in the bulk, we would see the area divergence at a later t .

Thus, we have seen that the area of the cross-sections of the global event horizon in the CS spacetime increases with time, with a logarithmic divergence. This implies that we cannot identify it with the entropy in the dual field theory. In the field theory, passing from the global BTZ black hole to the CS spacetime is just a conformal transformation, and the entropy of the fluid is invariant under conformal transformations. Thus, we expect the total entropy of the fluid flow corresponding to the CS spacetime to be the same as in the static fluid dual to the global BTZ black hole, independent of the spatial slice on the boundary we choose to measure it on. The point is that although the dual fluid flow is time-dependent, it is an ideal fluid, and in the absence of any viscous or dissipative effects we cannot have any entropy production (for a brief review see Appendix B). As a result we should have the field theory entropy being constant even in the CS spacetime.

We are thus led to propose that in dynamical spacetimes with ‘significant’ time variations, one should not associate the area of the event horizon to the entropy of the dual field theory. This point of view seems natural from studies of entanglement entropy in AdS/CFT [25] and also in dynamical black hole spacetimes which are out of the hydrodynamic regime [26]. The physical argument is simply that the event horizon is a teleological object. We need to know the entire future evolution of the classical geometry in order to determine the location of the horizon. On the other hand, even in a system perturbed away from equilibrium, one expects that entropy is produced locally, i.e., it makes sense to extract the entropy in some domain of the fluid by analyzing the local evolution equations. One should not have to evolve the fluid globally for all times before inferring the entropy production in some region. This suggests that in the gravitational description one should look for an appropriate quasi-local horizon whose area we can associate with the entropy. We will argue that in the CS spacetime the relevant object is the apparent horizon.

This might appear to contradict the argument of [16] where it was proposed that it is the event horizon area that corresponds to the field theory entropy. However, as discussed in §1, in that case it was assumed that the fluid settles down at late times to a stationary solution, which is not the case for the CS spacetime. Indeed if the dissipative physics drives the evolution then we expect that at late times the event horizon coincides with the apparent horizon,¹⁵ and moreover for slow variations which are required for the hydrodynamic description this situation will pertain for all times. However, the CS spacetime doesn’t fit into the slow variation paradigm despite the ideal fluid description and hence leads to a distinct behaviour of event and apparent horizons.

¹⁵This statement relies on a sensible choice of foliation of the spacetime, as the apparent horizons are foliation dependent. We return to this issue in the Discussion section and Appendix D.

3.4 Apparent horizon for the CS spacetime

We have seen that the event horizon in the CS geometry deviates significantly from the global event horizon, because of the restriction to \mathcal{I}_{CS}^+ . We would now like to see where the apparent horizon in the CS geometry lies. As the apparent horizon is a more local concept, we might expect it to be less affected by the boundary restriction, and this is indeed what we find.

The notion of apparent horizon is intimately tied to the notion of trapped surfaces. Recall that a closed, co-dimension two spacelike surface \mathcal{S} (which for the CS_{2+1} geometry is just a closed curve) is trapped if both (ingoing and outgoing) future-directed null geodesic congruences emanating normal to the surface \mathcal{S} have negative expansions, i.e. the areas of the ‘wavefronts’ for these null congruences decrease in time. Physically, the presence of such a trapped surface indicates a region of strong gravitational effects, since ordinarily, e.g. in flat spacetime or AdS, the ingoing congruence contracts but the outgoing congruence expands. Indeed, for spacetimes with complete scri satisfying certain positive energy conditions, any trapped surface must be contained within a black hole. Moreover, the existence of a trapped surface implies the existence of a spacetime singularity. A surface is marginally trapped if the outgoing null congruence has zero expansion, while the ingoing congruence has negative expansion. There are several (strictly-speaking distinct) notions of “apparent horizon”.¹⁶ In the numerical relativity community, an apparent horizon on a given spacelike slice is defined as the outermost marginally trapped surface on that slice. In mathematical relativity, an apparent horizon is usually taken to be the boundary of the union of all trapped points (points lying on a trapped surface), again on a given spacelike slice. However, subject to certain smoothness conditions, which are satisfied by our CS spacetime, the apparent horizon so defined does indeed have vanishing outgoing expansion [29].

The important subtlety to note about both of these definitions is that a given spacetime geometry does not by itself specify the location of the apparent horizon; we first need to specify a foliation of the spacetime, with respect to which we can then define the apparent horizon.¹⁷ In the present case, the physically relevant foliation is one corresponding to constant Poincaré time slices.

We could now proceed to find the apparent horizon by an explicit computation (see Appendix C). However, this is a difficult calculation, so it is better to argue on general grounds. Since the Schwarzschild-AdS spacetime satisfies the energy conditions and has a complete \mathcal{I}^+ , the apparent horizon on any spacelike slice must lie inside or on the event horizon. The position of the apparent horizon on any given slice does not depend on the rest of the foliation, so we can view a given constant t slice as part of a t -foliation of the CS, or as

¹⁶An excellent review of the various quasi-local horizons is found in [30].

¹⁷In fact, as demonstrated in [31], even the Schwarzschild black hole spacetime admits (sufficiently bizarre) foliations for which there are no trapped surfaces at all, so that there is no apparent horizon.

part of a foliation of the global BTZ spacetime (obtained by translating the given slice by τ rather than t). In the latter case, the relevant event horizon is not the CS event horizon which ‘flares out’, but rather the global event horizon, which stays at constant radius $r = r_+$ for all times. This means that the apparent horizon cannot lie outside the $r = r_+$ surface. Since the $t = 0$ slice in Poincaré coordinates coincides with the $\tau = 0$ slice in BTZ coordinates, where the apparent horizon of the static black hole coincides with its event horizon, we know the apparent horizon on this slice coincides with the global horizon at $r = r_+$. Furthermore, by the area theorem pertaining to the apparent horizon, this apparent horizon cannot recede in the future since its area cannot decrease. This, combined with the previous argument that the apparent horizon cannot lie outside the global event horizon, forces the apparent horizon to coincide with the global event horizon for all times, which immediately implies that its area is constant.¹⁸ The above argument is confirmed by an explicit calculation of the expansion of the null normals in Appendix C.

Since the area of the apparent horizon is constant, it can be identified with the entropy of the dual field theory. This example thus provides strong evidence that the entropy of the field theory fluid should in general be identified with the area of the apparent horizon rather than that of the event horizon. The large difference between the event horizon and the apparent horizon in this spacetime arises from the global structure – specifically the restriction to \mathcal{I}_{CS}^+ . This indicates that it is the teleological nature of the event horizon which makes it inappropriate for a dual description of the field theory entropy. The apparent horizon, like the entropy, is determined by considering the situation at a moment in time (on a single spacelike slice). Furthermore, subject to the appropriate energy conditions being satisfied the apparent horizon also respects the second law, i.e., the area along cross-sectional slices of the apparent horizon is constrained to be non-decreasing. Hence, it is appropriate to use the pull-back¹⁹ of the area of the apparent horizon to the boundary and regard it as a Boltzmann H-function.

4 Discussion

In this paper we have discussed two distinct hydrodynamic solutions from a gravitational viewpoint. We analyzed the global causal properties of the spacetimes dual to Bjorken flow and the conformal soliton flow. Our bulk analysis confirms that both these spacetimes fit

¹⁸ In fact, below and in Appendix D we will argue more generally that an apparent horizon of a spacetime with compact Killing horizon must coincide with this Killing horizon for any foliation which allows complete sections of the Killing horizon.

¹⁹Although in [16] it was convenient to pull-back the horizon area form along ingoing null geodesics, in the present case of the apparent horizon being static, it doesn’t matter exactly how we pull back the area form to the boundary.

into the fluid-gravity paradigm, albeit in a somewhat novel fashion.

The first one, the boost invariant Bjorken flow, was shown to have a regular event horizon and is a genuine regular black hole spacetime. Our analysis here relied on explicitly constructing the null generators of the event horizon order by order in the late time expansion, consistent with the perturbation expansion of the gravity solution. This provides a final consistency check of the late time expansion as a gradient expansion used in the hydrodynamic context.

Our second example, the conformal soliton flow, which from the bulk standpoint might seem more prosaic, in fact proved more interesting. The solution was just a coordinate transformation of a known static solution, the Schwarzschild-AdS black hole. However, here we encountered a surprising result for the event horizon as seen by an observer living in the boundary Minkowski space. We constructed the event horizon by explicitly delineating the boundary of the past of \mathcal{I}_{CS}^+ , the future infinity accessible to such a boundary observer. While \mathcal{I}_{CS}^+ is not a complete future null infinity, it is of relevance in the field theory (or hydrodynamic) description. We can think of the event horizon thus defined as the Poincaré horizon for the black hole spacetime. It is a dynamical null hypersurface, whose spatial cross-section area diverges logarithmically for positive Poincaré times. We then argued that for sensible foliations of the spacetime, including the constant Poincaré time slices, the apparent horizon on the slices will coincide with the global BTZ event horizon at $r = r_+$.

This example shows that in strongly time-dependent settings, it is the apparent horizon, not the event horizon, which encodes the field theory entropy in the gravitational dual. One might have thought that the event horizon demarcates the region of spacetime that the asymptotic (or boundary) observer can see and therefore its area should encode the number of active degrees of freedom that are relevant for the field theory dynamics and hence is a measure of entropy. On the other hand, the event horizon is teleological as its determination requires knowledge of the entire future evolution of the spacetime. Thus by using its area as a measure of entropy we would be predicting a drastic non-locality in the field theory dynamics. We therefore argue that we should instead use the area of the apparent horizon as a measure for the entropy of the field theory.

Let us briefly revisit the issue of foliation-dependence of apparent horizons. In a case of genuinely dynamical spacetimes where the apparent horizon is a dynamical (spacelike) horizon, general foliations which don't respect spherical symmetry generically lead to distinct apparent horizons. One might expect this to be the case even for static black holes, since certain sufficiently bizarre slicings can remove the apparent horizon entirely (as demonstrated for the Schwarzschild black hole by [31]). One might therefore think that by continuity any non-spherical slicing would deform the position of the apparent horizon. However, this is not the case for static black holes. Above we have argued that in the Poincaré slicing, the apparent horizon of the CS geometry coincides with the global event horizon at $r = r_+$; but our argument did not depend on any specifics of the slicing. In fact, for *any* foliation which

admits a complete slice of the global event horizon, it is easy to show that the apparent horizon must coincide with the global event horizon. This can of course be confirmed by explicit calculation of the expansion; but a much simpler argument is presented in Appendix D. The way that the example of [31] gets around this is that their slicing does not allow a complete slice of the future event horizon. This result is consistent with our expectations from the field theory: for time-dependence which is trivial in this sense, the entropy should not change.

On the other hand, for genuinely dynamical situations, where the geometry has no Killing horizons, one might worry that the location, and thereby the area, of the apparent horizon is foliation-dependent. A-priori, this is not necessarily inconsistent with the field theory expectations: different boundary slicings may lead to different entropy because the field theory state at different times is different. Nevertheless, this intriguing picture of apparent horizon area giving the entropy of the boundary state still leaves more to be understood in the genuinely dynamical context: On the one hand, the area of a particular slice of the apparent horizon depends on where the slice intersects the horizon – for expanding apparent horizon, slices intersecting the horizon at later times will have larger areas. On the other hand, in the boundary theory, the entropy should depend only on the state at a particular boundary time-slice (not necessarily constant Poincare time, but at the same time not be dependent on the behaviour of the bulk slice away from the boundary). This seems to imply that our bulk prescription has more freedom or ambiguity in defining the entropy than that afforded by the boundary theory. One possibility is that there is a preferred foliation of the bulk, such as a zero-mean-curvature slicing, on which one is supposed to evaluate the area. However, we don't have a good physical justification for this option. A simpler resolution to this puzzle is that in the regime where the concept of entropy is meaningful, the horizon has to be evolving slowly enough that there is negligible difference between the areas of all slices of horizon which end on the same boundary time-slice. This is essentially the same picture as that advocated in [5, 16], except that here we use it for apparent horizon rather than the event horizon. In effect the field theory on the boundary should achieve local equilibrium in order for entropy to be a meaningful observable.

A general lesson from this discussion seems to be that while in situations near equilibrium, the event and apparent horizons are reasonably close and therefore provide adequate diagnostic measures for the field theory entropy, in far-from-equilibrium scenarios or those with strong modifications to the boundary conditions, we should use the quasi-local apparent horizon as opposed to the event horizon to measure the entropy. It would be interesting to establish this for generic situations in the context of the AdS/CFT correspondence.

Note added in v2: We have been rather glib in our terminology, mainly because the context in which we are working is sufficiently mild. Technically speaking, what we called “apparent horizon” should really be referred to as “dynamical horizon” (in case of a spacelike

co-dimension 1 surface), or “isolated horizon” (in case of a null surface). The BF spacetime exemplifies the former, which is the more generic case, whereas the CS spacetime gives the latter. We should emphasize that generally an apparent horizon is defined as a co-dimension 2 surface, on a given leaf of foliation, corresponding to the outermost marginally trapped surface or the boundary of trapped points, and as such, the set of apparent horizons on all leaves of the foliation need not form a smooth co-dimension 1 surface in the full spacetime.²⁰ This supplies further reason why one can not assert that “entropy is given by the area of apparent horizon” in full generality, since the entropy is expected to be smoothly varying in time, whereas the area of apparent horizon can jump discontinuously. We would however view the foliation-dependence to be a more worrying issue, as explained in the Discussion above, since it arises under much milder conditions than the actual discontinuities in apparent horizon.

Acknowledgements

It is a pleasure to thank Roberto Emparan, David Garfinkle, Carsten Gundlach, Michal Heller, Gary Horowitz, Kasper Peeters, Larry Yaffe and Marija Zamaklar for useful discussions. VH and MR would like to thank LPTHE (Paris), MIT, and KITP for hospitality during the course of this work. MR would also like to acknowledge the hospitality of CERN. PF is supported STFC Rolling Grant. VEH, MR and SFR are supported in part by STFC. VEH and MR are supported in part by the National Science Foundation under the Grant No. NSF PHY05-51164.

A Conformal solitons in higher dimensions

Consider the global Schwarzschild-AdS_{d+1} black hole whose metric is given as

$$ds^2 = -f(r) d\tau^2 + \frac{dr^2}{f(r)} + r^2 d\Omega_{d-1}^2, \quad (\text{A.1})$$

with the function $f(r)$ being

$$f(r) = 1 + r^2 - \left(\frac{r_+}{r}\right)^{d-2} (1 + r_+^2) \quad (\text{A.2})$$

We choose to parameterize the metric on the \mathbf{S}^{d-1} keeping manifest $SO(d-1)$ rotational isometry, i.e.,

$$d\Omega_{d-1}^2 = d\phi^2 + \sin^2 \phi d\Omega_{d-2}^2. \quad (\text{A.3})$$

²⁰In fact for certain discontinuous cases these two definitions don’t necessarily coincide.

This makes it easier to make contact with the discussion in §3 for the BTZ spacetime, since now Fig. 2 illustrates the behaviour in the $\{r, \tau, \phi\}$ space (where every point now represents a \mathbf{S}^{d-2} of radius $r \sin \phi$). The event horizon of this spacetime is at $r = r_+$.

To restrict consideration to the Poincaré patch of this spacetime, we proceed as before by a similar coordinate transformation to (3.3):

$$z = \frac{1}{\sqrt{r^2 + 1} \cos \tau + r \cos \phi}, \quad t = \frac{\sqrt{r^2 + 1} \sin \tau}{\sqrt{r^2 + 1} \cos \tau + r \cos \phi}, \quad \mathbf{x}_{d-1} = \frac{r \sin \phi \boldsymbol{\Omega}_{d-2}}{\sqrt{r^2 + 1} \cos \tau + r \cos \phi}. \quad (\text{A.4})$$

with $\boldsymbol{\Omega}_{d-2}$ denoting a unit vector on \mathbf{S}^{d-2} . The resulting CS_{d+1} spacetime is qualitatively similar to that discussed in §3. We now wish to determine the event horizon for this CS_{d+1} spacetime. This is achieved as discussed in §3.2 by working out the null geodesics bounding the past of \mathcal{I}_{CS}^+ .

Taking into account the symmetries of the background (A.1), the equations for a null geodesic congruence respecting the $SO(d-1)$ rotational symmetric are

$$\dot{r}^2 = 1 - \frac{\ell^2}{r^2} f(r), \quad \dot{\tau} = \frac{1}{f(r)}, \quad \dot{\phi} = \frac{\ell}{r^2}, \quad (\text{A.5})$$

where $\dot{}$ denotes the derivative with respect to the affine parameter λ . We have normalized the affine parameter by choosing to set the energy of the geodesic to unity, and we identify each geodesic by the parameter ℓ corresponding to the angular momentum.

We are interested in the null geodesics that can reach \mathcal{I}^+ when sent from some $r > r_+$. The only novelty in this calculation relative to the BTZ case is that the effective potential for the radial motion (writing the geodesic equation as $\dot{r}^2 + V_{\text{eff}}(r) = 0$),

$$V_{\text{eff}}(r) = -1 + \frac{\ell^2}{r^2} f(r), \quad (\text{A.6})$$

has a distinct maximum associated with the unstable photon orbit at

$$r_{\text{ph}} = r_+ \left(\frac{d}{2} (1 + r_+^2) \right)^{\frac{1}{d-2}}. \quad (\text{A.7})$$

Geodesics emanating from $r < r_{\text{ph}}$ will make it out to the boundary only if $V_{\text{eff}}(r_{\text{ph}}) < 0$, which translates to an upper bound on the angular momentum $\ell < \ell_{\text{max}}$

$$\ell_{\text{max}}^2 = \frac{r_{\text{ph}}^2}{r_{\text{ph}}^2 + \left(1 - \frac{2}{d}\right)}. \quad (\text{A.8})$$

For $r > r_{\text{ph}}$ however we can have $0 \leq \ell \leq 1$ as usual. Massless particles have to overcome the gravitational centripetal barrier to escape to infinity to \mathcal{I}^+ .

Despite this complication, it is straightforward to integrate (A.5) to find the geodesics explicitly. For the special case of $d = 4$ (i.e., Schwarzschild-AdS₄₊₁) one can write closed form expressions using $u = 1/r$ as:²¹

$$\begin{aligned}\phi(u, \ell) &= \pm \frac{1}{\alpha r_+ \sqrt{1+r_+^2}} F \left[\arcsin \left(\frac{u}{\alpha} \right), \frac{\beta}{\alpha} \right], \\ \tau(u, \ell) &= \pi - \frac{1}{\beta \ell r_+ \sqrt{1+r_+^2} (1+2r_+^2)} \left\{ \frac{1}{\zeta^2} \Pi \left[\arcsin \left(\frac{u}{\alpha} \right), -\frac{\alpha^2}{\zeta^2}, \frac{\alpha}{\beta} \right] + \frac{1}{\xi^2} \Pi \left[\arcsin \left(\frac{u}{\alpha} \right), -\frac{\alpha^2}{\xi^2}, \frac{\alpha}{\beta} \right] \right\},\end{aligned}\tag{A.9}$$

where $F(\varphi, k)$ and $\Pi(\varphi, n, k)$ are the incomplete elliptic integrals of the first and third kind respectively, and we have defined the constants

$$\begin{aligned}\alpha &= \frac{1}{2r_+^2(1+r_+^2)} \left(1 + \frac{1+2r_+^2}{\ell} \sqrt{\ell^2 - \ell_{\max}^2} \right), & \beta &= \frac{1}{2r_+^2(1+r_+^2)} \left(1 - \frac{1+2r_+^2}{\ell} \sqrt{\ell^2 - \ell_{\max}^2} \right), \\ \zeta &= \frac{1}{\sqrt{1+r_+^2}}, & \xi &= \frac{1}{r_+}.\end{aligned}\tag{A.10}$$

The event horizon determined by this null congruence qualitatively looks similar to the BTZ case as illustrated in Fig. 3.

B The conformal soliton flow and hydrodynamics

We illustrate the fact that the conformal soliton flow does not lead to entropy production. As explained in the text, the coordinate transformation (3.3) when restricted to the boundary is a conformal transformation. In this appendix we review briefly the conformal transformation of the hydrodynamic variables.

In d spacetime dimensions, under a conformal transformation of the background metric, the stress tensor transforms homogeneously with conformal weight $d + 2$. In particular, we have the transformation:

$$g_{\mu\nu} = e^{2\phi} \tilde{g}_{\mu\nu}, \quad T^{\mu\nu} = e^{-(d+2)\phi} \tilde{T}^{\mu\nu}.\tag{B.1}$$

which implies that the velocity and thermodynamic variables transform as

$$u^\mu = e^{-\phi} \tilde{u}^\mu, \quad \rho = e^{-d\phi} \tilde{\rho}, \quad P = e^{-d\phi} \tilde{P}, \quad T = e^{-\phi} \tilde{T}, \quad s = e^{-(d-1)\phi} \tilde{s}\tag{B.2}$$

where s is the entropy density of the fluid. Note that the total entropy S is clearly invariant under conformal transformations.²² One further quantity we will be interested in is the

²¹We have picked the branch cuts in evaluating the integrals so as to obtain manifestly real expressions for τ and ϕ in (A.9).

²²The entropy is dimensionless and therefore doesn't depend on the conformal frame. Entropy density on the other hand behaves like inverse spatial volume as it must.

entropy current, which for an ideal fluid takes the form²³

$$j_s^\mu = s u^\mu, \quad (\text{B.3})$$

and transforms under conformal transformations as

$$j_s^\mu = e^{-d\phi} \tilde{j}_s^\mu. \quad (\text{B.4})$$

For simplicity we will take the tilded variables to correspond to the global BTZ solution. We have then in the global coordinates

$$\tilde{u}^a = \left(\frac{\partial}{\partial \tau} \right)^a, \quad \tilde{T} = \frac{r_+}{2\pi}, \quad \tilde{s} = \frac{1}{4} r_+, \quad (\text{B.5})$$

leading to an entropy current vector

$$\tilde{j}_s^a = \frac{1}{4} r_+ \left(\frac{\partial}{\partial \tau} \right)^a, \quad (\text{B.6})$$

which clearly is divergence free $\tilde{\nabla}_a \tilde{j}_s^a = 0$.

Transforming to the Poincaré coordinates we find the velocity 1-form

$$u = \frac{1}{2W} \left((1 + x^2 + t^2) dt - 2tx dx \right), \quad (\text{B.7})$$

which leads to an entropy current

$$j_s^a = \frac{r_+}{8W^2} \left((1 + x^2 + t^2) \left(\frac{\partial}{\partial t} \right)^a - 2tx \left(\frac{\partial}{\partial x} \right)^a \right), \quad (\text{B.8})$$

which again turns out to satisfy

$$\nabla_a j_s^a = 0 \quad (\text{B.9})$$

which is what we expect. The system stays an ideal fluid in the Poincaré frame. While there is some spatio-temporal variation of the energy density and temperature, there is no entropy production. This is of course as expected, an ideal fluid stays ideal in all conformal frames. While we have worked out the result for the BTZ spacetime, it is easy to check that the same result holds in higher dimensions. In fact from the discussion in Appendix A it is clear that the transverse $SO(d-1)$ symmetry of the \mathbf{S}^{d-2} ensures that we are essentially dealing with very similar physics.

²³For the moment we are going to ignore corrections to this coming from dissipative terms which of course lead to entropy production.

C Apparent horizon in the Poincaré slicing of BTZ

In this Appendix we derive the apparent horizon for the Poincaré patch of the BTZ spacetime i.e., the CS_3 spacetime. We have given a general argument in §3.4 to claim that the apparent horizon for the CS spacetime coincides with the event horizon in the global BTZ spacetime, and in Appendix D we generalize this still further, to argue that for any stationary black hole, in any foliation admitting a complete section of the horizon, the apparent horizon must coincide with the event horizon. However, to provide more concrete insight, here we proceed by explicit calculation.

The coordinate transformation in the bulk (3.3) mapping the global BTZ to CS, turns out to be too cumbersome for computation. In order to implement a conformal transformation on the boundary to map the fluid on $\mathbf{R}^{1,1}$ to the cylinder $\mathbf{S}^1 \times \mathbf{R}^1$, we only require a bulk coordinate transformation that reduces to the appropriate conformal mapping (3.5). As a simpler bulk diffeomorphism consider:

$$z_s = \frac{1}{r(\cos \tau + \cos \phi)}, \quad t_s = \frac{\sin \tau}{\cos \tau + \cos \phi}, \quad x_s = \frac{\sin \phi}{\cos \tau + \cos \phi}. \quad (\text{C.1})$$

We will use (C.1) and find the apparent horizon of the $t = \text{const.}$ slices.²⁴

As a further simplification, we will only consider two slices: one at $t_s = 0$, which is a symmetric slice and another at $t_s = \infty$. We will argue that these slices have a marginally trapped surface at $r = r_+$ which will be the apparent horizon we seek. Since the location of the apparent horizon is the same on these two distinct slices, using the monotonicity property of apparent horizon area, we conclude that the apparent horizon must lie at $r = r_+$ for all t_s . Moreover to keep the equations manageable we will write them out in the global coordinates, with the transformation (C.1) being used only to specify the slices.

The time symmetric slice: The $t_s = 0$ slice, Σ_0 , clearly coincides with the $\tau = 0$ slice in global coordinates. On this surface we consider an arbitrary closed curve γ given by $r = g(\phi)$, which is our ansatz for a trapped surface. The outgoing null normal to the spacetime co-dimension two surface γ is given as

$$k_a = -\sqrt{g^2 - r_+^2} (d\tau)_a + \frac{1}{\sqrt{g^2 - r_+^2 + \frac{(g')^2}{g^2}}} ((dr)_a - g'(d\phi)_a) \quad (\text{C.2})$$

Using the induced metric on γ :

$$q_{ab} dx^a dx^b = \left[g^2 + \frac{(g')^2}{g^2 - r_+^2} \right] d\phi^2, \quad (\text{C.3})$$

²⁴Strictly speaking the constant t_s slices in the coordinates (C.1) differ from the constant Poincaré time slices in (3.3). Nevertheless, the foliations are sufficiently similar that we can trust that the apparent horizons in the two coordinate charts with $t_s = \text{const}$ spacelike slices have the same qualitative features.

the expansion of the outgoing null normals $\theta \equiv q^{ab}\nabla_a k_b$ can be computed to be

$$\theta_0 = \frac{g^2(g^2 - r_+^2)^2}{[g^2(g^2 - r_+^2) + (g')^2]^{\frac{5}{2}}} [(g')^2 + g^2(g^2 - r_+^2) - g g'']. \quad (\text{C.4})$$

We want to find a marginally trapped surface for which the outgoing null geodesics are non-expanding. This requires us to have $\theta_0 = 0$ which gives us a second order non-linear ordinary differential equation for the curve $r = g(\phi)$. We will now argue that in fact the curve is simply $g(\phi) = r_+$, which coincides with the location of the global event horizon.

Along any curve γ , consider the outermost point p , where the function $g(\phi)$ attains its maximal value. Then g will satisfy $g'(p) = 0$ and $g''(p) < 0$, which allows us to bound the expansion of the outgoing null geodesics at this point:

$$\theta_\gamma(p) = \frac{\sqrt{g^2 - r_+^2}}{g} \left[1 - \frac{g''}{g(g^2 - r_+^2)} \right] \Big|_p \geq 0, \quad \text{for } g > r_+ > 0. \quad (\text{C.5})$$

This implies that if γ is a trapped surface, then its furthest point cannot lie outside r_+ . On the other hand, if we consider a circle \mathcal{C} , for which $g' = g'' = 0$, then we find that for all points on \mathcal{C} , the expansion of the outgoing null geodesics is given by

$$\theta_{\mathcal{C}} = \frac{\sqrt{g^2 - r_+^2}}{g}, \quad (\text{C.6})$$

which is always positive if $g > r_+$ and becomes zero when $g = r_+$. (Note that if we take \mathcal{C} to enclose the whole of γ and intersect it at p outside r_+ , then $\theta_{\mathcal{C}} \leq \theta_\gamma(p)$, since γ is more curved than \mathcal{C} at p .) We conclude then that, since no trapped surface can reach outside $r = r_+$, whereas the circle $g = r_+$ is marginally trapped, the curve $g(\phi) = r_+$ gives the apparent horizon. Therefore, we have argued that in the $t = 0$ slice of the conformal soliton geometry, the apparent horizon coincides with the global event horizon.

The late Poincaré time slice: From (C.1), we find that the $t = \infty$ slice, Σ_∞ , is given by the condition

$$\cos \tau + \cos \phi = 0. \quad (\text{C.7})$$

Following the same steps as before, we consider an arbitrary closed curve on Σ_∞ and compute the expansion of the outgoing null geodesics to this curve. We find

$$\theta_\infty = \frac{r_+(g^2 - r_+^2)^2}{[r_+^2(g^2 - r_+^2) + (g')^2]^{\frac{5}{2}}} [g(g')^2 + g r_+^2(g^2 - r_+^2) - g_+^2 g'']. \quad (\text{C.8})$$

Applying the same argument as in the previous case we conclude that the apparent horizon of the Σ_∞ slice is at $g = r_+$, which again coincides with location of the global event horizon. Therefore, since the area of the apparent horizon does not change with time, we conclude that the entropy in the field theory also stays constant, as expected.

General slicings: We have given in §3.4 a general argument for the apparent horizon to coincide with the global event horizon. Here we illustrate this by an explicit computation. To avoid obfuscating issues to do with foliation dependence of the apparent horizon, we will focus on slices which contain an entire spatial cross section of the global event horizon.

Consider a general timelike foliation of the Schwarzschild-AdS spacetime given by an arbitrary function

$$t_g = F(\tau, r, \phi) . \quad (\text{C.9})$$

We are interested in the nature of trapped surfaces lying on the spacelike surfaces defined by (C.9). We find it convenient to invert the relation (C.9) and express the global time coordinate τ as a function of the other variables;

$$\tau = \mathcal{F}(t_g; r, \phi) , . \quad (\text{C.10})$$

On each of the slices (C.10) consider the circles $r = \text{const}$. The outgoing null normal to any of these circles is given by

$$k_a = -\mathcal{N}(d\tau)_a + \left(\mathcal{N} \partial_r \mathcal{F} + \frac{r}{\mathcal{N}Q} \right) (dr)_a + \mathcal{N} \partial_\phi \mathcal{F} (d\phi)_a , \quad (\text{C.11})$$

where

$$\mathcal{N} = \sqrt{\frac{r^2(r^2 - r_+^2)}{r^2 - (r^2 - r_+^2) [r^2(r^2 - r_+^2)(\partial_r \mathcal{F})^2 + (\partial_\phi \mathcal{F})^2]}} , \quad Q = \sqrt{r^2 - (r^2 - r_+^2)(\partial_\phi \mathcal{F})^2} . \quad (\text{C.12})$$

While the general expression is unilluminating, for our purposes it suffices to argue that the surfaces $r = r_+$ are trapped. In order to establish this, we compute the expansion of these outgoing null normals for our test circles lying in the vicinity of the global event horizon, i.e., $r \sim r_+$. Assuming furthermore that \mathcal{F} and its derivatives are sufficiently smooth at $r = r_+$, we find

$$\theta = \frac{\sqrt{2} [r_+ + \partial_\phi^2 \mathcal{F}(r_+, \phi)] \sqrt{r - r_+}}{r_+^{\frac{3}{2}}} + \mathcal{O} \left((r - r_+)^{\frac{3}{2}} \right) \quad (\text{C.13})$$

near $r = r_+$. Therefore, we conclude that the surface $r = r_+$ is indeed trapped for general slicings of the spacetime.

D Apparent horizon coincides with Killing horizon

Recall that for general dynamical black hole spacetimes, the location of an apparent horizon is foliation dependent. Changing the foliation slightly will in general change the location of the apparent (or the so-called dynamical) horizon slightly. However, this is not the case for stationary black holes, or more generally black holes which have a Killing horizon. (Note

that for stationary black holes, the event horizon is a Killing horizon.) In this Appendix we will explain why an apparent horizon of a spacetime with compact Killing horizon must coincide with the Killing horizon for *any* foliation which allows complete sections of the Killing horizon.

The basic outline of the argument is the following: Any slice of a Killing horizon is a marginally trapped surface, since the outgoing null normals to any such slice of the horizon coincide with the horizon generators (due to the Killing horizon being null), and the horizon generators have zero expansion (because any spacelike slice of a Killing horizon has the same proper area). Moreover, this marginally trapped surface is the outermost one, since there cannot be trapped surfaces outside the event horizon. Hence for a slicing which admits a complete cross-section of the (future) event horizon, the apparent horizon necessarily coincides with the event horizon.

Let us now demonstrate the assertion that any complete slice of a Killing horizon is a marginally trapped surface using the example of 3-dimensional rotationally-invariant black hole. We proceed by first describing an arbitrary spacelike slice of the horizon in terms of its tangent vector, and then determining the null normals to this vector. Having obtained the null normals, we can then easily confirm that the outgoing null normal coincides with the horizon generators.

Since we wish to consider the geometry at the event horizon, let us write the metric more conveniently in ingoing Eddington coordinates:

$$ds^2 = g_{vv} dv^2 + 2 dv dr + g_{xx} dx^2 \quad (\text{D.1})$$

where the metric components g_{vv} and g_{xx} are functions of r which we don't need to specify for our argument. Suppose the event horizon lies on a constant r surface, $r = r_+$, where $g_{vv} = 0$. Then along any spacelike slice of the horizon, we can write the tangent vector as

$$s^a = \mathcal{N} \left(\frac{\partial}{\partial x} \right)^a + \mathcal{C} \left(\frac{\partial}{\partial v} \right)^a \quad (\text{D.2})$$

for some arbitrary coefficient \mathcal{C} (which can vary along the slice). In order for s^a to be unit-normalised, it suffices to let $\mathcal{N} = 1/\sqrt{g_{xx}(r = r_+)}$. Now, to solve for the null normal to our slice, we want to find a vector ξ^a which satisfies $\xi^a \xi_a = 0$ and $\xi^a s_a = 0$. Let

$$\xi^a = \left(\frac{\partial}{\partial v} \right)^a + \mathcal{A} \left(\frac{\partial}{\partial r} \right)^a + \mathcal{B} \left(\frac{\partial}{\partial t} \right)^a \quad (\text{D.3})$$

Then the null condition $\xi^a \xi_a = 0$ implies $g_{vv} + 2\mathcal{A} + \mathcal{B}^2 g_{xx} |_{r=r_+} = 2\mathcal{A} + \mathcal{B}^2/\mathcal{N}^2 = 0$, while the normal condition $\xi^a s_a = 0$ yields $\mathcal{C} g_{vv} + \mathcal{C}\mathcal{A} + \mathcal{N}\mathcal{B} g_{xx} |_{r=r_+} = \mathcal{C}\mathcal{A} + \mathcal{B}/\mathcal{N} = 0$. For any given \mathcal{C} , there exist two distinct solutions: either

$$\mathcal{A} = \mathcal{B} = 0, \quad (\text{D.4})$$

or

$$\mathcal{A} = -2/\mathcal{C}^2, \quad \mathcal{B} = 2\mathcal{N}/\mathcal{C}. \quad (\text{D.5})$$

Since in the latter solution, (D.5), the coefficient \mathcal{A} of $(\frac{\partial}{\partial r})^a$ is negative, the resulting ξ^a corresponds to ingoing null normals. This means that the first solution, (D.4), corresponds to the outgoing null normals. Thus we have found that for an arbitrary slice of the horizon, i.e. for any \mathcal{A} , the outgoing null normal is given by $\xi^a = (\frac{\partial}{\partial v})^a$, independently of \mathcal{A} . It is easy to see that if $(\frac{\partial}{\partial v})^a$ is a Killing vector, the Killing horizon generators are simply $(\frac{\partial}{\partial v})^a$, which are null on the horizon. This proves our first assertion, that the outgoing null normals to any slice of the Killing horizon coincide with the horizon generators.

Finally, the fact that the Killing horizon generators have zero expansion can be easily shown by noting that the proper area of the horizon remains constant along the generators, and moreover using similar arguments as above, this area is the same along any spacelike slice of the horizon; we leave this as an exercise for the reader.

References

- [1] J. D. Bjorken, “Highly Relativistic Nucleus-Nucleus Collisions: The Central Rapidity Region,” *Phys. Rev.* **D27** (1983) 140–151.
- [2] R. A. Janik and R. B. Peschanski, “Asymptotic perfect fluid dynamics as a consequence of AdS/CFT,” *Phys. Rev.* **D73** (2006) 045013, [arXiv:hep-th/0512162](#).
- [3] R. A. Janik and R. B. Peschanski, “Gauge / gravity duality and thermalization of a boost-invariant perfect fluid,” *Phys. Rev.* **D74** (2006) 046007, [arXiv:hep-th/0606149](#).
- [4] M. P. Heller, R. A. Janik, and R. Peschanski, “Hydrodynamic Flow of the Quark-Gluon Plasma and Gauge/Gravity Correspondence,” *Acta Phys. Polon.* **B39** (2008) 3183–3204, [arXiv:0811.3113 \[hep-th\]](#).
- [5] S. Bhattacharyya, V. E. Hubeny, S. Minwalla, and M. Rangamani, “Nonlinear Fluid Dynamics from Gravity,” *JHEP* **02** (2008) 045, [arXiv:0712.2456 \[hep-th\]](#).
- [6] D. T. Son and A. O. Starinets, “Viscosity, Black Holes, and Quantum Field Theory,” *Ann. Rev. Nucl. Part. Sci.* **57** (2007) 95–118, [arXiv:0704.0240 \[hep-th\]](#).
- [7] M. Van Raamsdonk, “Black Hole Dynamics From Atmospheric Science,” *JHEP* **05** (2008) 106, [arXiv:0802.3224 \[hep-th\]](#).
- [8] S. Bhattacharyya, R. Loganayagam, S. Minwalla, S. Nampuri, S. P. Trivedi, and S. R. Wadia, “Forced Fluid Dynamics from Gravity,” *JHEP* **02** (2009) 018, [arXiv:0806.0006 \[hep-th\]](#).

- [9] M. Haack and A. Yarom, “Nonlinear viscous hydrodynamics in various dimensions using AdS/CFT,” *JHEP* **10** (2008) 063, [arXiv:0806.4602 \[hep-th\]](#).
- [10] S. Bhattacharyya, R. Loganayagam, I. Mandal, S. Minwalla, and A. Sharma, “Conformal Nonlinear Fluid Dynamics from Gravity in Arbitrary Dimensions,” *JHEP* **12** (2008) 116, [arXiv:0809.4272 \[hep-th\]](#).
- [11] J. Erdmenger, M. Haack, M. Kaminski, and A. Yarom, “Fluid dynamics of R-charged black holes,” *JHEP* **01** (2009) 055, [arXiv:0809.2488 \[hep-th\]](#).
- [12] N. Banerjee, J. Bhattacharya, S. Bhattacharyya, S. Dutta, R. Loganayagam, and P. Surowka, “Hydrodynamics from charged black branes,” [arXiv:0809.2596 \[hep-th\]](#).
- [13] M. Haack and A. Yarom, “Universality of second order transport coefficients from the gauge-string duality,” [arXiv:0811.1794 \[hep-th\]](#).
- [14] J. Hansen and P. Kraus, “Nonlinear Magnetohydrodynamics from Gravity,” [arXiv:0811.3468 \[hep-th\]](#).
- [15] M. M. Caldarelli, O. J. C. Dias, and D. Klemm, “Dyonic AdS black holes from magnetohydrodynamics,” [arXiv:0812.0801 \[hep-th\]](#).
- [16] S. Bhattacharyya, V. E. Hubeny, R. Loganayagam, G. Mandal, S. Minwalla, T. Morita, M. Rangamani, and H. S. Reall, “Local Fluid Dynamical Entropy from Gravity,” *JHEP* **06** (2008) 055, [arXiv:0803.2526 \[hep-th\]](#).
- [17] P. Kovtun, D. T. Son, and A. O. Starinets, “Viscosity in strongly interacting quantum field theories from black hole physics,” *Phys. Rev. Lett.* **94** (2005) 111601, [arXiv:hep-th/0405231](#).
- [18] M. P. Heller and R. A. Janik, “Viscous hydrodynamics relaxation time from AdS/CFT,” *Phys. Rev.* **D76** (2007) 025027, [arXiv:hep-th/0703243](#).
- [19] R. Baier, P. Romatschke, D. T. Son, A. O. Starinets, and M. A. Stephanov, “Relativistic viscous hydrodynamics, conformal invariance, and holography,” *JHEP* **04** (2008) 100, [arXiv:0712.2451 \[hep-th\]](#).
- [20] P. Benincasa, A. Buchel, M. P. Heller, and R. A. Janik, “On the supergravity description of boost invariant conformal plasma at strong coupling,” *Phys. Rev.* **D77** (2008) 046006, [arXiv:0712.2025 \[hep-th\]](#).
- [21] M. P. Heller, P. Surowka, R. Loganayagam, M. Spalinski, and S. E. Vazquez, “On a consistent AdS/CFT description of boost-invariant plasma,” [arXiv:0805.3774 \[hep-th\]](#).

- [22] S. Kinoshita, S. Mukohyama, S. Nakamura and K. y. Oda, “A Holographic Dual of Bjorken Flow,” *Prog. Theor. Phys.* **121**, 121 (2009), [arXiv:0807.3797 \[hep-th\]](#).
- [23] S. Kinoshita, S. Mukohyama, S. Nakamura and K. y. Oda, “Consistent Anti-de Sitter-Space/Conformal-Field-Theory Dual for a Time-Dependent Finite Temperature System,” *Phys. Rev. Lett.* **102**, 031601 (2009), [arXiv:0901.4834 \[hep-th\]](#).
- [24] J. J. Friess, S. S. Gubser, G. Michalogiorgakis, and S. S. Pufu, “Expanding plasmas and quasinormal modes of anti-de Sitter black holes,” *JHEP* **04** (2007) 080, [arXiv:hep-th/0611005](#).
- [25] V. E. Hubeny, M. Rangamani, and T. Takayanagi, “A covariant holographic entanglement entropy proposal,” *JHEP* **07** (2007) 062, [arXiv:0705.0016 \[hep-th\]](#).
- [26] P. M. Chesler and L. G. Yaffe, “Horizon formation and far-from-equilibrium isotropization in supersymmetric Yang-Mills plasma,” [arXiv:0812.2053 \[hep-th\]](#).
- [27] K. Kajantie, J. Louko and T. Tahkokallio, “Gravity dual of 1+1 dimensional Bjorken expansion,” *Phys. Rev. D* **76**, 106006 (2007), [arXiv:0705.1791 \[hep-th\]](#).
- [28] K. Kajantie, J. Louko and T. Tahkokallio, “Isotropic AdS/CFT fireball,” *Phys. Rev. D* **78**, 126011 (2008), [arXiv:0809.4875 \[hep-th\]](#).
- [29] R. Wald, *General Relativity*. University of Chicago Press, 1984.
- [30] I. Booth, “Black hole boundaries,” *Can. J. Phys.* **83** (2005) 1073–1099, [arXiv:gr-qc/0508107](#).
- [31] R. M. Wald and V. Iyer, “Trapped surfaces in the Schwarzschild geometry and cosmic censorship,” *Phys. Rev. D* **44** (1991) no. 12, 3719–3722.